Letter

Failed excitonic quantum phase transition in $Ta_2Ni(Se_{1-x}S_x)_5$

Pavel A. Volkov , 1,* Mai Ye , 1,† Himanshu Lohani, Irena Feldman, Amit Kanigel, and Girsh Blumberg , 1,3,‡

1 Department of Physics and Astronomy, Rutgers University, Piscataway, New Jersey 08854, USA

2 Department of Physics, Technion - Israel Institute of Technology, Haifa 32000, Israel

3 National Institute of Chemical Physics and Biophysics, 12618 Tallinn, Estonia



(Received 22 April 2021; revised 28 November 2021; accepted 1 December 2021; published 10 December 2021)

We study the electronic phase diagram of the excitonic insulator candidates $Ta_2Ni(Se_{1-x}S_x)_5$ (x = 0, ..., 1) using polarization resolved Raman spectroscopy. Critical excitonic fluctuations are observed that diminish with x and ultimately shift to high energies, characteristic of a quantum phase transition. Nonetheless, a symmetry-breaking transition at finite temperatures is detected for all x, exposing a cooperating lattice instability that takes over for large x. Our study reveals a failed excitonic quantum phase transition, masked by a preemptive structural order.

DOI: 10.1103/PhysRevB.104.L241103

Introduction. One of the fascinating manifestations of interactions between electrons in solids is the emergence of electronic orders. The fluctuations close to the respective quantum critical points are also believed to be the drivers of a wealth of yet unexplained behaviors, including strange metallicity and high- T_c superconductivity [1–4]. In many cases (such as, e.g., nematic [5,6] or density-wave [7,8] orders) electronic order breaks the symmetries of the crystalline lattice and the corresponding transitions can be, symmetry-wise, identical to structural ones. This raises the question of the role of the interplay between electronic and lattice degrees of freedom in the ordering. Even in cases where the lattice only weakly responds to the transition [9,10], the critical temperatures [11,12] and quantum critical properties [13] can be strongly modified. Moreover, in a number of cases the origin of the order is still under debate [14–16], as the lattice may develop an instability of its own.

The electronic-lattice dichotomy has recently come to the fore in studies of Ta₂NiSe₅ [17–19]—one of the few candidate materials for the excitonic insulator (EI) phase [16,20–24]. The EI results from a proliferation of excitons driven by Coulomb attraction between electrons and holes in a semiconductor or a semimetal [25–29]. Ta₂NiSe₅ exhibits a phase transition at $T_c = 328$ K; while the pronounced changes in band structure [18], transport [19], and optical [30] properties are consistent with the ones expected for an EI, they allow an alternative interpretation in terms of a purely structural phase transition [31–34]. Indeed, the EI state in Ta₂NiSe₅ is expected to break mirror symmetries of the lattice due to the distinct symmetries of the electron and hole states forming the exciton [35], similar to a structural transition [31]. Intriguingly, substitution of Se with S has been shown to suppress T_c in transport experiments to zero [19], suggesting a possible quantum phase transition (QPT) at $x = x_c$ in Ta₂Ni(Se_{1-x}S_x)₅. Increasing x enhances the band gap in the electronic structure [36], which is known to suppress the EI [27,28], consistent with an EI QPT. On the other hand, the lattice degrees of freedom also evolve with x making it imperative to separately assess the roles of electronic and lattice degrees of freedom throughout the phase diagram of $Ta_2Ni(Se_{1-x}S_x)_5$.

Experimentally, this is a challenging task. As transitions caused by the lattice and electronic degrees of freedom break the same symmetries [31,35], their signatures may appear identical in thermodynamic (e.g., specific heat [19]) and symmetry-sensitive (x-ray diffraction [17]) probes, as well as in the single-electron spectra [18,32]. Probing the collective dynamics out of equilibrium could provide more information [33,34,37], but raises the question of whether the nonequilibrium state preserves the interaction between the structural and electronic modes intact [38]. Finally, due to the even-parity nature of the critical mode [39], the dipole selection rules forbid direct observation of the order parameter response in optical absorption [30]. A promising technique to address the near-equilibrium collective dynamics is polarization-resolved Raman scattering [39–41] that also allows us to detect symmetry breaking independently [42-44]. Furthermore, analysis of the Raman data [38,39] enables us to deduce the individual contributions of the lattice and electronic modes to the transition, making this technique unique in its scope.

In this Letter we use polarization-resolved Raman scattering to study the dynamics of electronic excitations throughout the phase diagram of $Ta_2Ni(Se_{1-x}S_x)_5$. We reveal the presence of low-energy excitonic modes that soften on cooling towards $T_c(x)$. This softening indicates that in the absence of lattice effects, a purely excitonic transition would have taken place at $T_{ex}(x)$, which we deduce to be smaller than $T_c(x)$. On increasing sulfur content x, $T_{ex}(x)$ is suppressed to negative values and for x = 1 low-energy excitons are no longer observed, as expected for an excitonic insulator quantum phase transition. However, the actual $T_c(x)$ remains finite for all x, implying the presence of a cooperating lattice instability, obscuring the suppression of the excitonic order. The study thus reveals a "failed" excitonic quantum phase transition in

^{*}pv184@physics.rutgers.edu

[†]mye@physics.rutgers.edu

[‡]girsh@physics.rutgers.edu

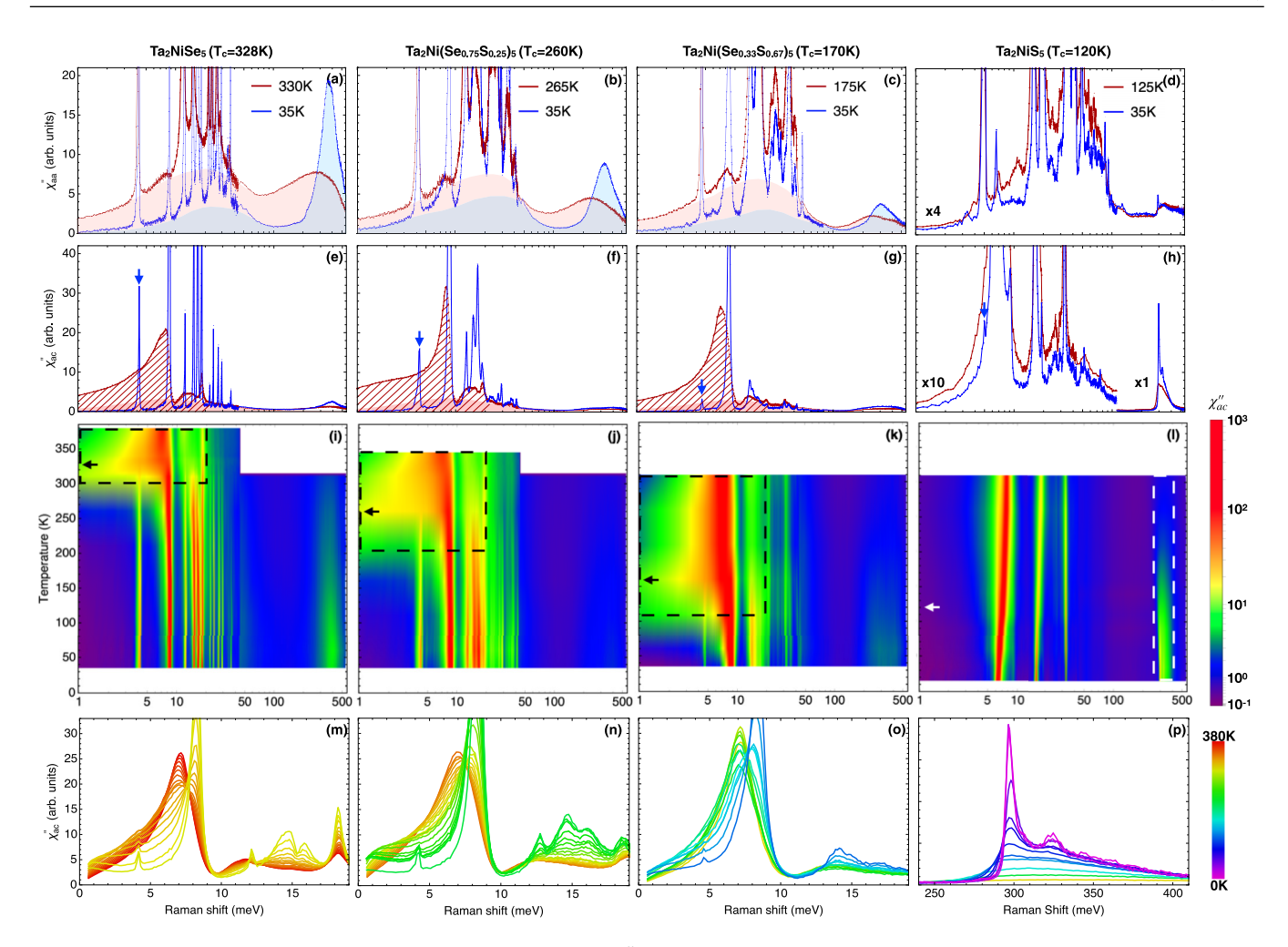


FIG. 1. Overview of the polarization-resolved Raman response $\chi''(\omega,T)$ in $\mathrm{Ta_2Ni}(\mathrm{Se_{1-x}S_x})_5$. (a)–(d) Response in aa polarization geometry corresponding to fully symmetric (A_g) excitations above (red) and below (blue) T_c for x=0–1. Shading highlights the bare electronic contribution to the response. (e) and (f) Same for ac geometry, probing the excitations with the symmetry of the order parameter (B_{2g}) for $T>T_c$ (red). Unlike aa geometry, phonons show an extremely anisotropic Fano line shape (hatching), indicating their strong interaction with the electronic continuum (red shading). For $T< T_c$ (blue) excitations observed in aa geometry above T_c appear (arrow) due to symmetry breaking. (i)–(l) Temperature dependence of $\chi''_{ac}(\omega,T)$; an enhancement at low energies near T_c (arrow) is observed for x=0,0.25,0.67. For x=1 no low-energy response is present. (m)–(p) Details of $\chi''_{ac}(\omega,T)$ for regions marked by dashed lines in (i)–(k). (m)–(o) Fano line shape of low-energy phonons due to interaction with electronic continuum. (p) High-energy peak due to an uncondensed exciton in $\mathrm{Ta_2NiS_5}$.

 $Ta_2Ni(Se_{1-x}S_x)_5$ masked by a preemptive structural order that takes over as the electronic instability is suppressed.

Experiment. We performed Raman scattering experiments on single crystals $Ta_2Ni(Se_{1-x}S_x)_5$ with varying Se/S content, grown using the chemical vapor transport (CVT) method [38,45]. The measurements were performed in a quasi-backscattering geometry on samples cleaved to expose the ac crystallographic plane with the 647 nm line from a Kr⁺ ion laser excitation, details presented in Ref. [38]. The selection rules in the high-temperature orthorhombic (point group D_{2h}) phase imply that ac polarization geometry probes excitations with B_{2g} symmetry (same as that of the order parameter), while aa geometry probes the fully symmetric A_g ones [38–41]. Below T_c , the point group symmetry is reduced to C_{2h} and the two irreducible representations merge, such that excitations from ac geometry above T_c may appear in aa geometry and vice versa. Their appearance allows us to determine T_c from the Raman spectra.

Data overview. Summarized temperature dependence of the Raman susceptibility $\chi''(\omega, T)$ is presented in Fig. 1. The samples with x = 0, 0.25, 0.67 show qualitatively similar spectra. At low energies, phonon peaks are observed on top of a smooth background, which we attribute to electronic excitations. On cooling, a pronounced redistribution of electronic intensity in a wide range of energies is observed, leading to a formation of a gaplike suppression followed by a high-energy feature, Figs. 1(a)–1(c). This feature at 380 meV for Ta₂NiSe₅ has been attributed to the coherence factors at the gap edge of an EI [39]. In ac geometry, a pronounced enhancement at low energies is evident close to T_c , consistent with critical mode softening near a second-order phase transition, Figs. 1(i)-1(k). In the same temperature region, the line shapes of the low-energy phonons show strongly asymmetric Fano form [Figs. 1(m)-1(o)]—a known signature of interaction with an electronic excitation continuum [38,39,46]. This indicates the presence of low-energy symmetry-breaking electronic

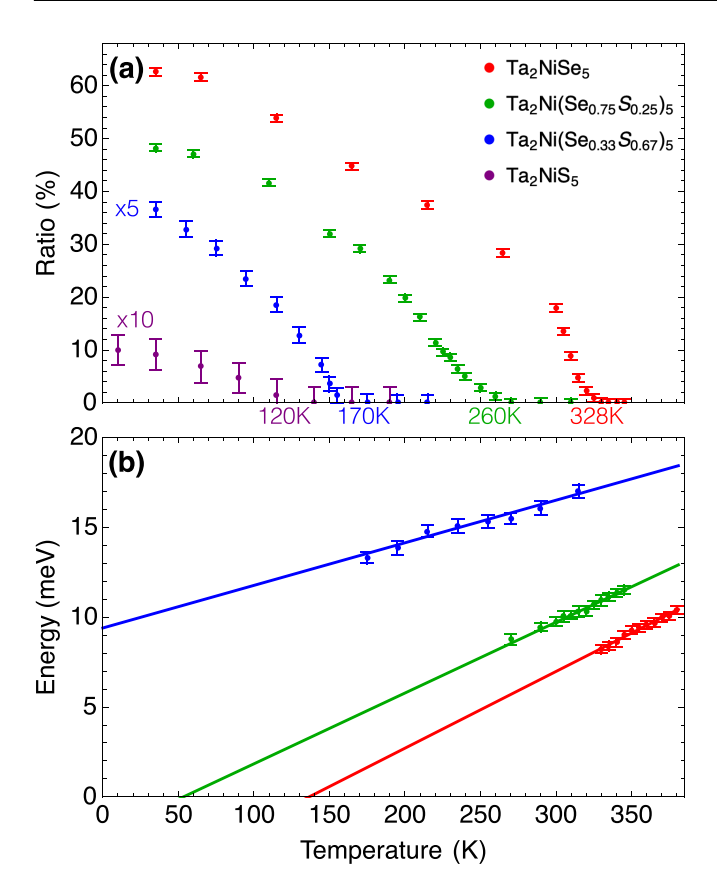


FIG. 2. The parameters deduced from the Raman response data, Fig. 1. (a) Integrated "leakage" intensity into ac scattering geometries of the lowest-energy A_g phonon mode labeled in Figs. 1(e)–1(h), normalized by the intensity in the dominant aa geometry. The mode's appearance in the ac scattering geometry below T_c implies the onset of symmetry breaking. (b) Excitonic energy $\Omega_e(T)$, Eq. (1), obtained from the Fano fits to the line shapes in Fig. 1. Lines represent linear fits to the points.

excitations that soften close to T_c . At low temperatures, the asymmetry disappears [Figs. 1(e)-1(g)], a behavior consistent with a gap opening in an EI. On increasing sulfur content x, the temperature where the strongest low-energy enhancement is observed progressively lowers [Figs. 1(i)-1(k)], and the A_g -symmetry feature at about 380 meV moves slightly to lower energy and becomes less pronounced.

The signatures for Ta_2NiS_5 (x=1) are rather different: in the ac geometry, low-energy electronic excitations are absent at all temperatures, indicating the presence of a direct gap. This implies that between x=0.67 and x=1 the electronic structure undergoes a Lifschitz transition from a semimetallic to an insulating one. The intensity in the aa geometry at low energies is also pronouncedly smaller than for the other samples and no broad high-energy peak is observed at low temperatures. On the contrary, a sharp feature at about 0.3 eV emerges in ac geometry on cooling below 100 K.

Symmetry-breaking transition. We address first the presence of a phase transition by studying the appearance of new modes in the broken-symmetry phase, as outlined above. In Fig. 2(a) we show the temperature dependence of such a "leakage" phonon intensity marked by arrow in

Figs. 1(e)-1(h). One can see the appearance of the leaked intensity below T_c in the pure Se case, as well as the decrease of T_c with S doping. Leakages of other modes appear below the same temperature T_c [38,45]. At low x the obtained values of T_c agree with the ones deduced from transport and specific heat measurements [19,38], Fig. 3. However, in contrast to the transport data reported in Ref. [19], we find that the symmetry-breaking transition persists for all compositions, although the leakage intensity is strongly suppressed with higher x. The latter suggests that the phase transition signatures in thermodynamic and transport measurements may become too weak to be observed at large x, especially since the system becomes more insulating with x. The structural signatures, e.g., the deviation of the monoclinic angle β from 90°, should be also strongly suppressed, being already weak at x = 0 [17].

The phase transition for x = 1, where no low-energy softening is observed [Fig. 1(1)], indicates a different transition mechanism. Below we analyze our data to elucidate the origin of the transition as a function of x.

Electronic contribution to the phase transition. We investigate first the soft-mode behavior observed for $x \leq 0.67$ [Figs. 1(i)-1(k)]. In particular, we analyze the asymmetric line shapes of the low-energy part of $\chi''_{ac}(\omega, T)$ around T_c [Figs. 1(m)-1(o)] using an extended Fano model [38,39]. The model assumes three phononic oscillators (which is the number of B_{2g} modes in the orthorhombic phase) interacting with a continuum of excitonic origin. The latter is expected to arise from the excitonic fluctuations in a semimetal, overdamped due to the allowed decay into particle-hole pairs. Close to the transition, the dynamics of the excitonic mode is governed by the time-dependent Landau equations [47–50]. Together with the standard oscillator dynamics of the phonons the system is described by

$$\{\partial_t + \Omega_e(T)\}\varphi + \sum_{i=1}^3 \tilde{v}_i \eta_i = 0,$$

$$\{\partial_t^2 + 2\gamma_i(T)\partial_t + \omega_{pi}^2(T)\}\eta_i + \tilde{v}_i \varphi = 0,$$
 (1)

where $\eta_{i=1,2,3}$ and φ are the collective coordinates (order parameters) of the optical phonons and excitons, respectively. $\Omega_e(T)$ is the characteristic energy of the excitonic fluctuations, $\omega_{pi}(T)$ and $\gamma_i(T)$ are the phonon frequencies and scattering rates, and a bilinear exciton phonon-coupling \tilde{v}_i is assumed. The linear response of the system Eq. (1) determines the Raman susceptibility. The resulting model [45] is a generalization of the standard Fano model [46] for Raman scattering in metals to the case of three phonons and the continuum response determined from the Landau theory, Eq. (1). The purely excitonic part of the response has then the form of a broad continuum $\chi''_{\rm cont}(\omega,T) \propto \frac{\omega}{\Omega_s^2(T)+\omega^2}$, in contrast to the Lorentzian phonon peaks. The interaction between the phonons and the excitonic continuum leads to an asymmetric broadening of the peaks [38], allowing us to capture the observed line shapes in great detail [38,39,45].

We now discuss the parameters deduced from the Fano model fits. The phonon frequencies $\omega_{pi}(T)$ do not soften near T_c [38], ruling out a zone-center phonon instability [31]. On the other hand, $\Omega_e(T)$ [Fig. 2(b), solid lines] consistently

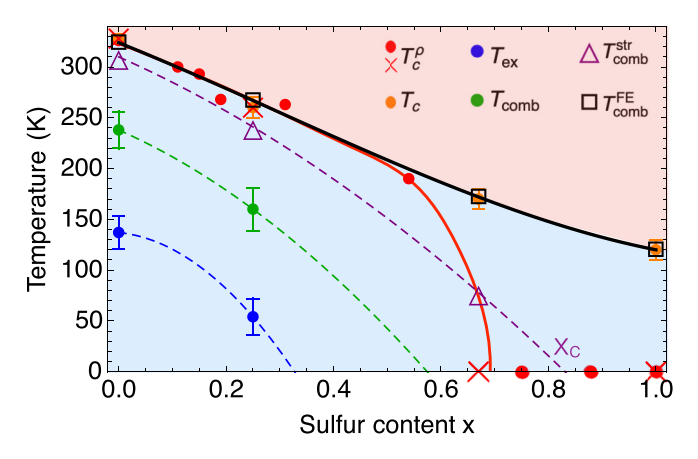


FIG. 3. Phase diagram of $Ta_2Ni(Se_{1-x}S_x)_5$. Orange points: The symmetry-breaking transition temperature $T_c(x)$ obtained from the onset of phonon intensity leakage, Fig. 2(a). Red points and crosses: $T_c^{\rho}(x)$ adapted from transport studies [19,38]. For low sulfur concentration x, the soft excitonic mode [Fig. 2(b)] would drive the transition at temperature $T_{\rm ex}(x)$ (blue points) that is enhanced to $T_{\rm comb}(x)$ by coupling to inter optical phonons (green points), and is further enhanced to $T_{\rm comb}^{\rm str}(x)$ by coupling to the B_{2g} strain (purple triangles). For large x, the excitonic softening is suppressed, while a ferroelastic instability leads to a finite $T_{\rm comb}^{\rm FE}(x)$ (black squares). In the absence of the lattice instability, a lattice-shifted electronic QPT would have occurred at x_c (dashed purple line). Additionally, in the same proximity, the band structure undergoes semimetal-to-semiconductor Lifschitz transition (see text).

softens above T_c for all semimetallic samples. The linear temperature dependence $\Omega_e(T) \sim T - T_{\rm ex}$ implies that a purely electronic transition would have taken place at $T_{\rm ex} < T_c$ for x = 0, 0.25 (Fig. 3, blue symbols). The strongly negative $T_{\rm ex}$ for x = 0.67 indicates that the exciton softening alone would not have led to a transition at this sulfur concentration.

The suppression of the excitonic instability with x is even more evident in Ta₂NiS₅ [Figs. 1(d), 1(h) and 1(1)], where the low-energy electronic response is altogether absent due to a direct band gap [36]. Instead, we observe a sharp B_{2g} symmetry mode at 0.3 eV [Fig. 1(p)], consistent with an in-gap exciton. It is followed by a weaker feature at 0.325 eV and an intensity "tail" at higher energies up to around 0.4 eV. The natural interpretation of the second peak is the second state of the Rydberg series (i.e., 2S exciton), while the highenergy intensity tail can be attributed, in analogy with optical absorption spectroscopy, to the Rydberg states of higher order and interband transitions [51,52] with possible contributions from phonon-assisted exciton transitions [53,54]. A leakage of the exciton features is also observed in aa geometry due to symmetry breaking, Fig. 1(d) [45]. On heating, all the features broaden and eventually smear out above 100 K. The increase of the linewidth of the excitonic features can be attributed to the interaction with acoustic and optical phonons [55].

Ferroelastic transition in Ta_2NiSe_5 . The presented observations show that the excitonic instability on its own cannot explain the occurrence of a transition for samples with large x, calling for a more careful consideration of the lattice effects. The most vivid is the case of Ta_2NiS_5 , where the excitonic response is confined to high energies [Fig. 1(p)]. Three B_{2g}

optical phonon modes [Fig. 1(1)], on the other hand, exhibit some (around 15% maximum) softening on cooling. However, their energies never soften below 6.5 meV, nor exhibit anomaly at the transition temperature 120 K. We note that the number of B_{2g} modes is restricted to three by the space group of the orthorhombic Ta_2NiS_5 , implying the absence of any other B_{2g} optical modes beyond those shown in Fig. 1(1). Consequently, an instability of zone center phonons in Ta_2NiS_5 [56] is ruled out by the data.

The only remaining option for the transition origin in Ta_2NiS_5 is an instability of the acoustic modes, i.e., ferroelasticity [57,58], driven by softening of the B_{2g} shear modulus $C_{ac}(T)$. Indeed, the acoustic modes are not observed directly in Raman due to their extremely low energies and weak coupling to light [38,59]. However, we will show now that the effects of the ferroelastic instability can be observed at x < 1 via its coupling to the low-energy excitons.

Electronic-structural phase diagram. We will now demonstrate that the entire phase diagram of $Ta_2Ni(Se_{1-x}S_x)_5$ can be understood by including the interaction between excitonic and lattice modes. As has been noted above, the bare excitonic transition temperature $T_{\rm ex}$ (Fig. 3, blue line) is significantly lower than the actual T_c . However, even the coupling of excitons with the otherwise inert optical phonons can affect the transition temperature. For a coupled excitonic-optical phonon system, the transition temperature $T_{\rm comb}(x)$ corresponds to the appearance of a zero-energy solution of Eq. (1) deduced from [45]:

$$\Omega_e[x, T_{\text{comb}}(x)] - \sum_i \frac{\tilde{v}_i^2}{\omega_{pi}^2[x, T_{\text{comb}}(x)]} = 0, \qquad (2)$$

where all the parameters of this equation are deduced from the Fano analysis of the Raman data, Figs. 1(m)-1(o), following Ref. [38]. The resulting temperature $T_{\rm comb}(x)$ is shown in Fig. 3 (green line). While higher than $T_{\rm ex}(x)$, there is still discrepancy with T_c : for example, $T_{\rm comb}(x=0.67)$ is negative, while the actual $T_c(x=0.67)$ is 170 K.

We now include the effects of coupling of the excitonic order parameter φ to the B_{2g} strain ε_{ac} (acoustic modes). A linear coupling between the two is allowed by symmetry [11,12,39] and leads to a further modified equation for the transition temperature [39,45]:

$$\Omega_{e}\left[x, T_{\text{comb}}^{\text{FE}}(x)\right] - \sum_{i} \frac{\tilde{v}_{i}^{2}}{\omega_{pi}^{2}\left[x, T_{\text{comb}}^{\text{FE}}(x)\right]} - \lambda^{2} /$$

$$\left[2C_{ac}\left(T_{\text{comb}}^{\text{FE}}\right)\right] = 0,$$
(3)

where λ and $C_{ac}(T)$ is the strain-exciton coupling constant and the B_{2g} is shear modulus, respectively. To capture the ferroelastic instability at x=1, we assume a Curie-Weiss behavior of the shear modulus $C_{ac}^{-1}(T)=C_{ac(0)}^{-1}+\frac{a}{T-120~\rm K}$. Using $\lambda^2 C_{ac(0)}^{-1}$ and $\lambda^2 a$ as fitting parameters, the observed $T_c(x)$ can be captured very accurately, see the black line in Fig. 3. Importantly, the effects of the ferroelastic softening become noticeable well before x=1. The purple dashed line $T_{\rm comb}^{\rm str}(x)$ obtained ignoring ferroelastic softening [i.e., taking $C_{ac}^{-1}(T)=C_{ac(0)}^{-1}$ in Eq. (3)]. The result deviates strongly from actual $T_c(x)$ already at x=0.67. Continuing the trend further suggests a complete suppression of ordering at

 $x_c \approx 0.8$ in the absence of ferroelasticity. At the same time, for low x, $T_{\rm comb}^{\rm str}(x)$ and $T_{\rm comb}^{\rm FE}(x)$ are almost indistinguishable, suggesting that ferroelasticity does not play a role in that case.

This picture bears important consequences for the physics of $Ta_2Ni(Se_{1-x}S_x)_5$. At low x, the transition is driven, to a good approximation, only by the excitonic softening. On increasing x, the lattice softening becomes more important, and for x = 1 the transition is purely ferroelastic. In the absence of ferroelasticity, an electronic QPT would have occurred at $x_c \approx 0.8$. We remind that the excitonic and lattice orders break the same symmetries in $Ta_2Ni(Se_{1-x}S_x)_5$. Consequently, no change in symmetry occurs as a function of x at low temperatures and a true QPT at T=0 is avoided (unlike the case of superconductivity emerging near quantum critical points). However, this does not preclude critical electronic fluctuations, associated with the "failed" QPT at $x_c \approx 0.8$ to be observed at sufficiently high temperatures (higher than the bare lattice transition temperature of 120 K) [13].

The presence of quantum critical fluctuations due to a failed excitonic OPT lends a natural explanation to the signatures of strong correlations observed in Ta₂NiSe₅. In particular, a filling-in, rather then closing of the gap in aa Raman spectra has recently been connected to strong electronic correlations [39]; moreover, ARPES studies [60] suggest the presence of "preformed excitons" well above T_c also characteristic of a correlated regime. Similar temperature evolution of aa spectra is also observed for the doped samples, Figs. 1(b) and 1(c). Interestingly, while the intensity of the coherent aa peak is suppressed with doping, as is expected from mean-field theory [61], the position of the peak changes only weakly. The latter behavior indicates strong correlations which get a natural explanation in terms of the quantum critical fluctuations from the failed QPT. Finally, ferroelasticity may be suppressed by strain [62] or pressure [19] raising the possibility to reveal the bare EI QPT at low temperatures. For a semimetallic band structure, the EI QPT has been predicted to lead to non-Fermi liquid behavior [63], mass enhancement [64], or emergence of superconductivity [65]. Interestingly, a superconducting dome near the end point of the monoclinic phase has been recently reported in Ta₂NiSe₅ under pressure [66].

Conclusions. In this work we used polarized Raman scattering to study the phase diagram of the excitonic insulator candidates $Ta_2Ni(Se_{1-x}S_x)_5$, disentangling the roles of structural and electronic ordering. We revealed a failed excitonic insulator quantum phase transition at $x_c \approx 0.8$, avoided due to a lattice instability below 120 K. At low sulfur content x we observed a soft excitonic mode driving the transition, while at large x this mode ultimately transforms into a high-energy exciton, unable to drive the transition. We further exclude the instability of optical phonons and demonstrate that a ferroelastic instability yields an explanation of the observed symmetry-breaking transition. While the excitonic quantum phase transition is avoided due to the low-temperature lattice instability, the associated critical fluctuations can still be present at high temperatures [13], explaining the correlation effects in Ta₂NiSe₅. Furthermore, selective control of the structural and excitonic instability by strain [62] or pressure [19] can turn $Ta_2Ni(Se_{1-x}S_x)_5$ into a platform to study the excitonic QPT at low temperatures as well as quantum critical ferroelasticity [67].

Acknowledgments. The authors acknowledge discussions with K. Haule. The spectroscopic work conducted at Rutgers (M.Y. and G.B.) was supported by the National Science Foundation (NSF) Grants No. DMR-1709161 and No. DMR-2105001. P.A.V. acknowledges the Postdoctoral Fellowship support from the Rutgers University Center for Materials Theory. The sample growth and characterization work conducted at the Technion was supported by the USA-Israel Binational Science Foundation (BSF) Grant No. 2020745 and by the Israel Science Foundation (ISF) Grant No. 1263/21 (H.L., I.F., and A.K.). H.L. was supported in part by a PBC fellowship of the Israel Council for Higher Education. The work at NICPB was supported by the European Research Council (ERC) under Grant Agreement No. 885413.

P.A.V. and M.Y. contributed equally to this project.

H. v. Löhneysen, A. Rosch, M. Vojta, and P. Wölfle, Fermiliquid instabilities at magnetic quantum phase transitions, Rev. Mod. Phys. 79, 1015 (2007).

^[2] M. Brando, D. Belitz, F. M. Grosche, and T. R. Kirkpatrick, Metallic quantum ferromagnets, Rev. Mod. Phys. 88, 025006 (2016).

^[3] D. J. Scalapino, A common thread: The pairing interaction for unconventional superconductors, Rev. Mod. Phys. 84, 1383 (2012).

^[4] T. Shibauchi, A. Carrington, and Y. Matsuda, A quantum critical point lying beneath the superconducting dome in iron pnictides, Annu. Rev. Condens. Matter Phys. 5, 113 (2014).

^[5] S. A. Kivelson, E. Fradkin, and V. J. Emery, Electronic liquidcrystal phases of a doped Mott insulator, Nature (London) 393, 550 (1998).

^[6] E. Fradkin, S. A. Kivelson, M. J. Lawler, J. P. Eisenstein, and A. P. Mackenzie, Nematic fermi fluids in condensed matter physics, Annu. Rev. Condens. Matter Phys. 1, 153 (2010).

^[7] G. Gruner, Density Waves in Solids (CRC Press, Boca Raton, FL, 2018).

^[8] S. A. Kivelson, I. P. Bindloss, E. Fradkin, V. Oganesyan, J. M. Tranquada, A. Kapitulnik, and C. Howald, How to detect fluctuating stripes in the high-temperature superconductors, Rev. Mod. Phys. 75, 1201 (2003).

^[9] J.-H. Chu, J. G. Analytis, K. De Greve, P. L. McMahon, Z. Islam, Y. Yamamoto, and I. R. Fisher, In-plane resistivity anisotropy in an underdoped iron arsenide superconductor, Science 329, 824 (2010).

^[10] R. M. Fernandes, A. V. Chubukov, and J. Schmalian, What drives nematic order in iron-based superconductors? Nat. Phys. 10, 97 (2014).

^[11] J.-H. Chu, H.-H. Kuo, J. G. Analytis, and I. R. Fisher, Divergent nematic susceptibility in an iron arsenide superconductor, Science 337, 710 (2012).

^[12] A. E. Böhmer, P. Burger, F. Hardy, T. Wolf, P. Schweiss, R. Fromknecht, M. Reinecker, W. Schranz, and C. Meingast,

- Nematic Susceptibility of Hole-Doped and Electron-Doped BaFe₂As₂ Iron-Based Superconductors from Shear Modulus Measurements, Phys. Rev. Lett. **112**, 047001 (2014).
- [13] I. Paul and M. Garst, Lattice Effects on Nematic Quantum Criticality in Metals, Phys. Rev. Lett. 118, 227601 (2017).
- [14] R. Comin and A. Damascelli, Resonant x-ray scattering studies of charge order in cuprates, Annu. Rev. Condens. Matter Phys. 7, 369 (2016).
- [15] D. Mou, A. Sapkota, H.-H. Kung, V. Krapivin, Y. Wu, A. Kreyssig, X. Zhou, A. I. Goldman, G. Blumberg, R. Flint, and A. Kaminski, Discovery of an Unconventional Charge Density Wave at the Surface of K_{0.9}Mo₆O₁₇, Phys. Rev. Lett. 116, 196401 (2016).
- [16] A. Kogar, M. S. Rak, S. Vig, A. A. Husain, F. Flicker, Y. I. Joe, L. Venema, G. J. MacDougall, T. C. Chiang, E. Fradkin, J. van Wezel, and P. Abbamonte, Signatures of exciton condensation in a transition metal dichalcogenide, Science 358, 1314 (2017).
- [17] F. D. Salvo, C. Chen, R. Fleming, J. Waszczak, R. Dunn, S. Sunshine, and J. A. Ibers, Physical and structural properties of the new layered compounds Ta₂NiS₅ and Ta₂NiSe₅, J. Less Common. Met. **116**, 51 (1986).
- [18] Y. Wakisaka, T. Sudayama, K. Takubo, T. Mizokawa, M. Arita, H. Namatame, M. Taniguchi, N. Katayama, M. Nohara, and H. Takagi, Excitonic Insulator State in Ta₂NiSe₅ Probed by Photoemission Spectroscopy, Phys. Rev. Lett. 103, 026402 (2009).
- [19] Y. F. Lu, H. Kono, T. I. Larkin, A. W. Rost, T. Takayama, A. V. Boris, B. Keimer, and H. Takagi, Zero-gap semiconductor to excitonic insulator transition in Ta_2NiSe_5 , Nat. Commun. 8, 14408 (2017).
- [20] J. Neuenschwander and P. Wachter, Pressure-driven semiconductor-metal transition in intermediate-valence $TmSe_{1-x}Te_x$ and the concept of an excitonic insulator, Phys. Rev. B **41**, 12693 (1990).
- [21] K. Rossnagel, On the origin of charge-density waves in select layered transition-metal dichalcogenides, J. Phys.: Condens. Matter 23, 213001 (2011).
- [22] L. Du, X. Li, W. Lou, G. Sullivan, K. Chang, J. Kono, and R.-R. Du, Evidence for a topological excitonic insulator in InAs/GaSb bilayers, Nat. Commun. 8, 1971 (2017).
- [23] Z. Li, M. Nadeem, Z. Yue, D. Cortie, M. Fuhrer, and X. Wang, Possible excitonic insulating phase in quantum-confined Sb nanoflakes, Nano Lett. **19**, 4960 (2019).
- [24] Z. Zhu, P. Nie, B. Fauqué, B. Vignolle, C. Proust, R. D. McDonald, N. Harrison, and K. Behnia, Graphite in 90 T: Evidence for Strong-Coupling Excitonic Pairing, Phys. Rev. X 9, 011058 (2019).
- [25] L. V. Keldysh and Y. Kopaev, Possible instability of the semimetallic state toward Coulomb interaction, Sov. Phys. Solid State 6, 2219 (1965).
- [26] W. Kohn, Excitonic Phases, Phys. Rev. Lett. 19, 439 (1967).
- [27] D. Jérome, T. M. Rice, and W. Kohn, Excitonic insulator, Phys. Rev. 158, 462 (1967).
- [28] B. I. Halperin and T. M. Rice, Possible anomalies at a semimetal-semiconductor transition, Rev. Mod. Phys. 40, 755 (1968).
- [29] W. Kohn and D. Sherrington, Two kinds of bosons and Bose condensates, Rev. Mod. Phys. 42, 1 (1970).
- [30] T. I. Larkin, A. N. Yaresko, D. Pröpper, K. A. Kikoin, Y. F. Lu, T. Takayama, Y.-L. Mathis, A. W. Rost, H. Takagi, B. Keimer,

- and A. V. Boris, Giant exciton Fano resonance in quasi-one-dimensional Ta₂NiSe₅, Phys. Rev. B **95**, 195144 (2017).
- [31] A. Subedi, Orthorhombic-to-monoclinic transition in Ta_2NiSe_5 due to a zone-center optical phonon instability, Phys. Rev. Mater. 4, 083601 (2020).
- [32] M. D. Watson, I. Marković, E. A. Morales, P. Le Fèvre, M. Merz, A. A. Haghighirad, and P. D. C. King, Band hybridization at the semimetal-semiconductor transition of Ta₂NiSe₅ enabled by mirror-symmetry breaking, Phys. Rev. Res. 2, 013236 (2020).
- [33] E. Baldini, A. Zong, D. Choi, C. Lee, M. H. Michael, L. Windgaetter, I. I. Mazin, S. Latini, D. Azoury, B. Lv, A. Kogar, Y. Wang, Y. Lu, T. Takayama, H. Takagi, A. J. Millis, A. Rubio, E. Demler, and N. Gedik, The spontaneous symmetry breaking in Ta₂NiSe₅ is structural in nature, arXiv:2007.02909.
- [34] H. Lu, M. Ross, J. ho Kim, H. Yavas, A. Said, A. Nag, M. Garcia-Fernandez, S. Agrestini, K. Zhou, C. Jia, B. Moritz, T. P. Devereaux, Z.-X. Shen, and W.-S. Lee, Evolution of the electronic structure in Ta₂NiSe₅ across the structural transition revealed by resonant inelastic x-ray scattering, Phys. Rev. B 103, 235159 (2021).
- [35] G. Mazza, M. Rösner, L. Windgätter, S. Latini, H. Hübener, A. J. Millis, A. Rubio, and A. Georges, Nature of Symmetry Breaking at the Excitonic Insulator Transition: Ta₂NiSe₅, Phys. Rev. Lett. 124, 197601 (2020).
- [36] Y. Chiba, T. Mitsuoka, N. L. Saini, K. Horiba, M. Kobayashi, K. Ono, H. Kumigashira, N. Katayama, H. Sawa, M. Nohara, Y. F. Lu, H. Takagi, and T. Mizokawa, Valence-bond insulator in proximity to excitonic instability, Phys. Rev. B 100, 245129 (2019).
- [37] D. Werdehausen, T. Takayama, M. Höppner, G. Albrecht, A. W. Rost, Y. Lu, D. Manske, H. Takagi, and S. Kaiser, Coherent order parameter oscillations in the ground state of the excitonic insulator Ta₂NiSe₅, Sci. Adv. 4, eaap8652 (2018).
- [38] M. Ye, P. A. Volkov, H. Lohani, I. Feldman, M. Kim, A. Kanigel, and G. Blumberg, Lattice dynamics of the excitonic insulator $Ta_2Ni(Se_{1-x}S_x)_5$, Phys. Rev. B **104**, 045102 (2021).
- [39] P. A. Volkov, M. Ye, H. Lohani, I. Feldman, A. Kanigel, and G. Blumberg, Critical charge fluctuations and emergent coherence in a strongly correlated excitonic insulator, npj Quantum Mater. 6, 52 (2021).
- [40] K. Kim, H. Kim, J. Kim, C. Kwon, J. S. Kim, and B. J. Kim, Direct observation of excitonic instability in Ta₂NiSe₅, Nat. Commun. **12**, 1969 (2021).
- [41] G. Blumberg, Comment on "Direct observation of excitonic instability in Ta₂NiSe₅", arXiv:2103.03073.
- [42] H.-H. Kung, R. Baumbach, E. Bauer, V. Thorsmølle, W.-L. Zhang, K. Haule, J. Mydosh, and G. Blumberg, Chirality density wave of the "hidden order" phase in URu₂Si₂, Science 347, 1339 (2015).
- [43] M. Ye, E. W. Rosenberg, I. R. Fisher, and G. Blumberg, Lattice dynamics, crystal-field excitations, and quadrupolar fluctuations of YbRu₂Ge₂, Phys. Rev. B **99**, 235104 (2019).
- [44] S.-F. Wu, W.-L. Zhang, L. Li, H.-B. Cao, H.-H. Kung, A. S. Sefat, H. Ding, P. Richard, and G. Blumberg, Coupling of fully symmetric As phonon to magnetism in Ba(Fe_{1-x}Au_x)₂As₂, Phys. Rev. B **102**, 014501 (2020).
- [45] See Supplemental Material at http://link.aps.org/supplemental/ 10.1103/PhysRevB.104.L241103 for the details of crystal

- growth and characterization, Raman measurements, and analysis, which includes Refs. [19,38,39,42,46–54,68–72].
- [46] M. V. Klein, Electronic Raman scattering, in *Light Scattering in Solids I*, edited by M. Cardona (Springe, Berlin, 1983), Vol. 8, Chap. 4, pp. 147–202.
- [47] N. Goldenfeld, Lectures on Phase Transitions and the Renormalization Group (CRC Press, Boca Raton, FL, 2018).
- [48] I. K. Schuller and K. E. Gray, Time-dependent Ginzburg– Landau: From single particle to collective behavior, J. Supercond. Novel Magn. 19, 401 (2006).
- [49] R. Yusupov, T. Mertelj, V. V. Kabanov, S. Brazovskii, P. Kusar, J.-H. Chu, I. R. Fisher, and D. Mihailovic, Coherent dynamics of macroscopic electronic order through a symmetry breaking transition, Nat. Phys. 6, 681 (2010).
- [50] A. Zong, P. E. Dolgirev, A. Kogar, E. Ergeçen, M. B. Yilmaz, Y.-Q. Bie, T. Rohwer, I.-C. Tung, J. Straquadine, X. Wang, Y. Yang, X. Shen, R. Li, J. Yang, S. Park, M. C. Hoffmann, B. K. Ofori-Okai, M. E. Kozina, H. Wen, X. Wang *et al.*, Dynamical Slowing-Down in an Ultrafast Photoinduced Phase Transition, Phys. Rev. Lett. 123, 097601 (2019).
- [51] R. J. Elliott, Intensity of optical absorption by excitons, Phys. Rev. 108, 1384 (1957).
- [52] H. Haug and S. W. Koch, Quantum Theory of the Optical and Electronic Properties of Semiconductors (World Scientific, Singapore, 2009).
- [53] Y. Toyozawa, Interband effect of lattice vibrations in the exciton absorption spectra, J. Phys. Chem. Solids 25, 59 (1964).
- [54] B. Segall and G. D. Mahan, Phonon-assisted recombination of free excitons in compound semiconductors, Phys. Rev. 171, 935 (1968).
- [55] S. Rudin, T. L. Reinecke, and B. Segall, Temperature-dependent exciton linewidths in semiconductors, Phys. Rev. B 42, 11218 (1990).
- [56] L. Windgätter, M. Rösner, G. Mazza, H. Hübener, A. Georges, A. J. Millis, S. Latini, and A. Rubio, Common microscopic origin of the phase transitions in Ta₂NiS₅ and the excitonic insulator candidate Ta₂NiSe₅, arXiv:2105.13924.
- [57] E. K. Salje, Ferroelastic materials, Annu. Rev. Mater. Res. 42, 265 (2012).
- [58] Not to be confused with ferroelectricity, usually driven by a soft optical mode [73].
- [59] Y. Gallais and I. Paul, Charge nematicity and electronic Raman scattering in iron-based superconductors, C. R. Phys. 17, 113 (2016).
- [60] K. Seki, Y. Wakisaka, T. Kaneko, T. Toriyama, T. Konishi, T. Sudayama, N. L. Saini, M. Arita, H. Namatame, M. Taniguchi,

- N. Katayama, M. Nohara, H. Takagi, T. Mizokawa, and Y. Ohta, Excitonic Bose-Einstein condensation in Ta₂NiSe₅ above room temperature, Phys. Rev. B **90**, 155116 (2014).
- [61] In a two-band model of the EI $\chi''_{aa}(\omega) \sim \nu_0 \sqrt{2W/(\omega 2W)}$ [39], where ν is the density of states above T_c and W is the interband hybridization, which is the order parameter for pure EI [35].
- [62] M. S. Ikeda, T. Worasaran, J. C. Palmstrom, J. A. W. Straquadine, P. Walmsley, and I. R. Fisher, Symmetric and antisymmetric strain as continuous tuning parameters for electronic nematic order, Phys. Rev. B 98, 245133 (2018).
- [63] X.-Y. Pan, J.-R. Wang, and G.-Z. Liu, Quantum critical phenomena of the excitonic insulating transition in two dimensions, Phys. Rev. B **98**, 115141 (2018).
- [64] J.-R. Wang, G.-Z. Liu, X. Wan, and C. Zhang, Quantum criticality of the excitonic insulating transition in the nodal-line semimetal ZrSiS, Phys. Rev. B 101, 245151 (2020).
- [65] P. A. Volkov and S. Moroz, Coulomb-induced instabilities of nodal surfaces, Phys. Rev. B 98, 241107(R) (2018).
- [66] K. Matsubayashi, H. Okamura, T. Mizokawa, N. Katayama, A. Nakano, H. Sawa, T. Kaneko, T. Toriyama, T. Konishi, Y. Ohta, H. Arima, R. Yamanaka, A. Hisada, T. Okada, Y. Ikemoto, T. Moriwaki, K. Munakata, A. Nakao, M. Nohara, Y. Lu et al., Hybridization-gap formation and superconductivity in the pressure-induced semimetallic phase of the excitonic insulator Ta₂NiSe₅, J. Phys. Soc. Jpn. 90, 074706 (2021).
- [67] M. Zacharias, I. Paul, and M. Garst, Quantum Critical Elasticity, Phys. Rev. Lett. 115, 025703 (2015).
- [68] A. Nakano, K. Sugawara, S. Tamura, N. Katayama, K. Matsubayashi, T. Okada, Y. Uwatoko, K. Munakata, A. Nakao, H. Sagayama, R. Kumai, K. Sugimoto, N. Maejima, A. Machida, T. Watanuki, and H. Sawa, Pressure-induced coherent sliding-layer transition in the excitonic insulator Ta₂NiSe₅, IUCrJ 5, 158 (2018).
- [69] P. G. Klemens, Anharmonic decay of optical phonons, Phys. Rev. 148, 845 (1966).
- [70] J. Yan, R. Xiao, X. Luo, H. Lv, R. Zhang, Y. Sun, P. Tong, W. Lu, W. Song, X. Zhu, and Y. Sun, Strong electron–phonon coupling in the excitonic insulator Ta₂NiSe₅, Inorg. Chem. 58, 9036 (2019).
- [71] W. Hayes and R. Loudon, *Scattering of Light by Crystals* (Dover, London, 2004).
- [72] U. Fano, Effects of configuration interaction on intensities and phase shifts, Phys. Rev. 124, 1866 (1961).
- [73] W. Cochran, Crystal stability and the theory of ferroelectricity, Adv. Phys. **9**, 387 (1960).